Journal of Structural Geology 32 (2010) 172–183

Contents lists available at ScienceDirect

Journal of Structural Geology

journal homepage: www.elsevier.com/locate/jsg

Cross-section restoration: A tool to simulate deformation. Application to a fault-propagation fold from the Cantabrian fold and thrust belt, NW Iberian Peninsula

Massimiliano Masini [1], Mayte Bulnes, Josep Poblet*

Departamento de Geología, Universidad de Oviedo, C/Jesús Arias de Velasco s/n, 33005 Oviedo, Spain

ARTICLE INFO

Article history:
Received 23 December 2008
Received in revised form
15 October 2009
Accepted 3 November 2009
Available online 18 November 2009

Keywords:
Deformation
Cross-section restoration
Fault-propagation fold
Layer-parallel shear
Cantabrian fold and thrust belt
Small-scale structures

ABSTRACT

Simulation of deformation in sections across tectonic structures can provide important information about the present-day state of such structures. A technique for simulation of deformation, based on cross-section restoration, is presented. The deformation parameters are calculated through a model that provides information in numerical format and the results are illustrated overlapping gridded images and diagrams on top of the sections across the structures in order to visualize their geological significance. The validity of this method has been proved through its application to a structure formed in a contractional regime. The structure analyzed is located in the Cantabrian Mountains, NW Iberian Peninsula, and consists of a fault-propagation fold made up of Carboniferous limestones. The excellent outcrop of this structure allowed a complete geological cross-section reconstruction, and a detailed structural and kinematic analysis in order to obtain an accurate restoration. The results furnished by the restoration technique about the deformation values and patterns are in agreement with small-scale structures observed in the field as well as with the geometry and kinematics of the structure.

1. Introduction

Knowing the deformation undergone by beds involved in tectonic structures is an important aim for structural geologists from the purely scientific point of view but also from the economic point of view since a large number of disciplines are interested in understanding the distribution and evolution of deformation in rocks (hydrocarbon, mining and ground water exploration, engineering geology, sub-surface storage of fluids, seismicity, etc.). Direct methods to measure deformation employ strain markers present in the rocks (fossils, fossil traces or different types of particles) such as those methods which construct strain ellipses using geometrical parameters measured from several lines on a plane (Ramsay, 1967; Ragan, 1985; Ramsay and Huber, 1987), the R/φ method (Ramsay, 1967; Dunnet, 1969), the "all-object-separation" plot (Fry, 1979a,b) and analysis of fibrous mineral overgrowths (Durney and Ramsay, 1973; Hedlund et al., 1994) amongst others. Unfortunately, in many folded/faulted regions it is not always possible to obtain deformation data since strain markers are absent, they are poorly distributed or they are not accessible (bad quality outcrops, sub-surface or offshore structures). One way to overcome this drawback consists of using techniques to simulate deformation which may be employed as predictive tools of deformation architecture in natural geological structures. These methods do not require collecting rock samples from the geological bodies analyzed because they deal with geological maps, cross-sections and/or 3D geological surfaces. Some of these techniques are curvature analysis of folded surfaces (e.g., Lisle, 1994; Samson and Mallet, 1997; Roberts, 2001), forward modelling (e.g., Thorbjornsen and Dunne, 1997; Bastida et al., 2003; Ormand and Hudleston, 2003; Allmendinger et al., 2004), restoration (e.g., Erickson et al., 2000; Hennings et al., 2000; Rouby et al., 2000; Dunbar and Cook, 2003; Moretti et al., 2007), restoration plus forward modelling (e.g., Allmendinger, 1998; Sanders et al., 2004; Poblet and Bulnes, 2007), etc.

Here we present a method similar to that of Erickson et al. (2000), Hennings et al. (2000), Rouby et al. (2000), Dunbar and Cook (2003), and Moretti et al. (2007), since they employ restoration to quantify different parameters that characterise the deformation undergone by rocks in folded/faulted regions. The strategy consists of introducing circular strain markers in a deformed cross-section, subsequently restoring the section together with the strain markers, and finally obtaining the strain ellipses (one for each strain marker) through application of

* Corresponding author. Tel.: +34 98 5109548; fax: +34 98 5103103.
E-mail address: jpoblet@geol.uniovi.es (J. Poblet).
[1] Now at YPF, Mendoza, Argentina.

0191-8141/$ – see front matter © 2009 Elsevier Ltd. All rights reserved.
doi:10.1016/j.jsg.2009.11.002

a mathematical model. The strain parameters are calculated in numerical format and the results are illustrated through graphical outputs displayed on top of the sections across the geological structures, which may be compared with the orientation and distribution of tectonic features such as minor-scale folds and fractures, structural fabrics, etc.

The predictive capabilities of the method are shown through its application to a fault-propagation fold developed over a thrust fault in the Bodón Structural Unit (Cantabrian Zone, NW Iberian Peninsula) affecting Carboniferous limestones. This fault-related fold is an example of a contractional tectonic structure, where geological data quality, and the excellent outcrop and accessibility allowed us to carry out a complete structural analysis in order to verify the method presented here. The fact that the stratigraphic sequence is well-known and that the structure is tilted, so that almost the whole structure is exposed and only a small amount of data extrapolation is needed to complete the geometry of the structure, makes it an excellent candidate to be studied in detail. In addition, the analysis of this natural example furnished information on the deformation undergone by different portions of fault-propagation folds related to thrusts.

The main goals pursued here are (a) show a practical application of the method using 2D sections across geological structures and (b) provide additional insight about deformation in fault-related folds developed over thrust faults.

2. Methodology

The methodology presented in this paper is based on the following procedure:

(a) construction of a retro-deformable geological cross-section parallel to the tectonic transport direction using all the available surface and sub-surface data;
(b) introduction of strain markers along the geological section, so that the size, density and distribution of the markers are a function of the features of the structure or region to be analyzed, the precision of the results one would like to obtain and the occurrence of specific areas in which high deformation amounts are suspected or have a particular geological significance;
(c) partial or total restoration of the geological section including strain markers;
(d) application of a mathematical transformation to the restored strain markers in order to calculate the orientation of the semi-axes and lines of no finite deformation of the deformation ellipses, and the magnitudes of ellipse ellipticity and layer-parallel strain derived from each strain marker;
(e) data contouring in order to interpolate deformation parameters in between strain markers;
(f) results display (contour/colour images of amount of ellipticity, diagrams showing orientations of ellipse semi-axes, etc.) onto the present-day, deformed geological cross-section;
(g) comparison of the cross-section including the deformation simulation with the deformed, geological cross-section including second-order structures to check whether the deformation parameters and patterns simulated are in accordance with the type, orientation and motion along the small-scale structures, and therefore, the deformation simulation is geologically reasonable; and
(h) use of the geological cross-section including the deformation simulation as a predictive tool for those regions in which not enough data are available, e.g., hidden portions of the structures in the sub-surface or offshore, poor seismic imaging or bad quality outcrops of some parts of the structure.

If the deformation simulation does not agree with the second-order structures present in the region and/or some anomalies or artefacts are detected in the deformation simulation, the following parameters must be checked and the procedure must be totally or partially repeated depending on the error encountered (Bulnes and Poblet, 1999): quality of the (a) geological data collected in the outcrop, sub-surface and/or offshore; (b) structural interpretation and (c) cross-section construction; (d) orientation of the section line; (e) position and dip of the pin and loose lines; (f) restoration algorithm(s) employed; (g) plane strain assumption; (h) size, density and/or position of the strain markers; (i) data interpolation algorithm(s) used; and/or (j) influence of parameters not considered such as vertical/horizontal compaction amongst others.

The method described above may be applied to different types of structures developed in contractional, extensional, inversion tectonics, etc., settings in which the distribution of strain along the folded/faulted layers may occur through different mechanisms such as layer-parallel shear, vertical/inclined shear, etc. In the natural example analyzed here, layer-parallel shear was the main mechanism, a common mode of distribution of deformation in sedimentary sequences involved in different types of structures formed under contractional conditions in upper crustal domains. This is the reason why the mathematical model developed below is in accordance with the geometrical properties of layer-parallel shear. The mathematical strategy is based on solving an equation system represented by 2×2 matrixes. In the departure state, that is the present-day, geological cross-section, circular strain markers are included and symbolized by circles with unit radius (Fig. 1). Each strain marker is defined by a local coordinate system with origin in the centre of the circle and is constrained by four points P_1, P_2, P_3 and P_4 defining a square with coordinates P_1:(0,1), P_2:(1,1), P_3:(1,0) and P_4:(0,0). When the present-day, geological cross-section, including circular strain markers, is restored each circle becomes an ellipse and the original coordinates of the points that constrain the circles change. The ellipses obtained in the restoration are reciprocal strain ellipses.

Knowing the original and the final coordinates of at least two points that define each strain marker, determining the parameters of the strain ellipse produced in natural deformations requires the application of an algebraic model (Fig. 1). For small portions of a section across a structure, the deformation is assumed to be homogeneous. Under these conditions, the eulerian equations of transformation of points enable calculating the strain ellipses using the departure state (present-day, geological cross-section) and the final state (restored, geological cross-section):

$$\begin{cases} X_1 = b_{11}x_1 + b_{12}x_2 \\ X_2 = b_{21}x_1 + b_{22}x_2 \end{cases}, \tag{1}$$

where the deformed and the undeformed state are represented by two coincident coordinate systems (x_1, x_2) (spatial coordinates) and (X_1, X_2) (material coordinates). The coefficients b_{ij} can be calculated solving the equation system (1), which is constituted by the matrix b (spatial deformation gradient) (see Malvern, 1969, pp. 156–157):

$$b = \begin{pmatrix} b_{11} & b_{12} \\ b_{21} & b_{22} \end{pmatrix}, \tag{2}$$

Using the layer-parallel shear assumption, $\det b = 1$ (no area variation) and the matrix of the Cauchy deformation tensor c is given by (see Malvern, 1969, p. 158):

$$c = b_T \cdot b = \begin{pmatrix} c_{11} & c_{12} \\ c_{21} & c_{22} \end{pmatrix}, \tag{3}$$

where b_T is the transposed matrix of b.

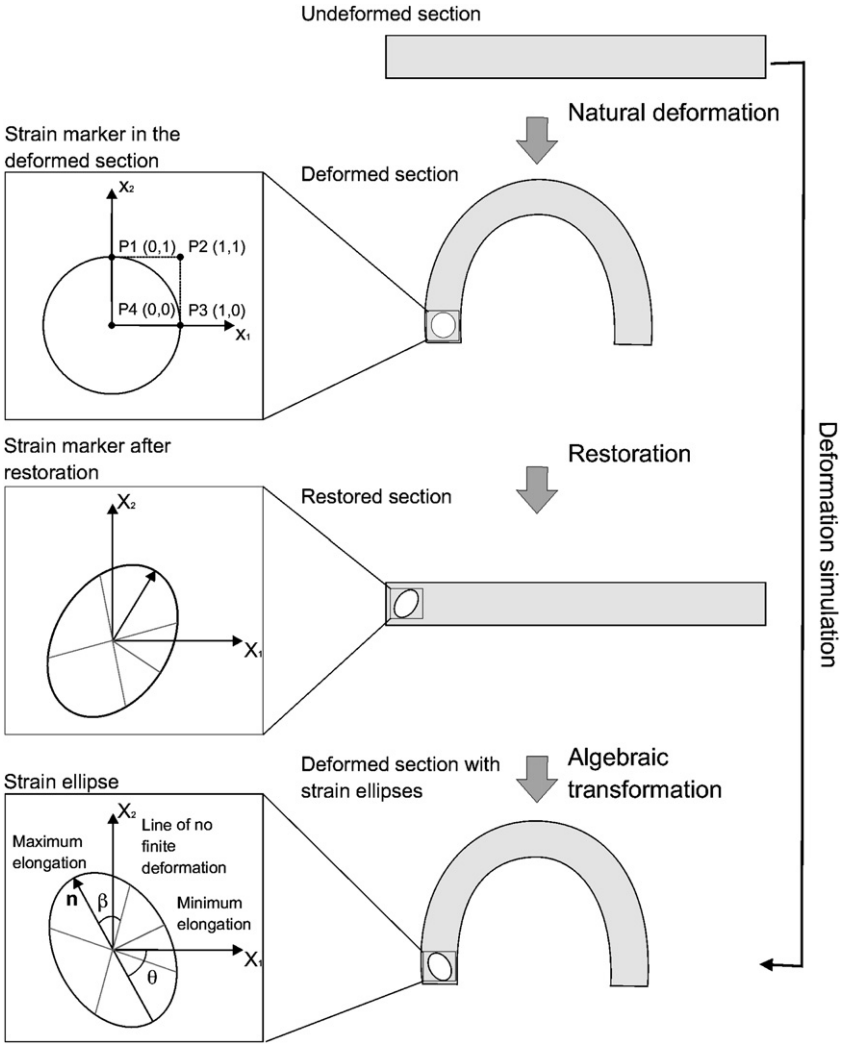

Fig. 1. Schematic illustration of the deformation simulation using cross-section restoration. Undeformed circle markers are placed onto the deformed, present-day cross-section. The initial circles are constrained by four points forming a unit square referred to a local coordinate system with origin in the centre of the circle. In the restored section the new coordinates of these points are used to calculate the strain parameters and to simulate the deformation on the present-day cross-section.

The matrix c is symmetrical; its characteristic equation is:

$$\lambda'^2 - i_1\lambda' + i_2 = 0, \tag{4}$$

where:

$$i_1 = c_{11} + c_{22} \tag{5}$$

and

$$i_2 = c_{11}c_{22} - c_{12} \tag{6}$$

are the invariants of the tensor c.

The roots of Eq. (4) give the principal reciprocal quadratic elongations, λ'_1 and λ'_2. From them the magnitudes of maximum and minimum stretch of the strain ellipse (Fig. 1) are given by:

$$\sqrt{\lambda_1} = \frac{1}{\sqrt{\lambda'_1}} \tag{7}$$

and

$$\sqrt{\lambda_2} = \frac{1}{\sqrt{\lambda'_2}} \tag{8}$$

To decipher the orientation of the strain ellipse the following equation is needed:

$$\begin{cases} (c_{11} - \lambda'_1)\cdot n_1 + c_{12}\cdot n_2 = 0 \\ c_{12}\cdot n_1 + (c_{22} - \lambda'_1)\cdot n_2 = 0 \end{cases}, \tag{9}$$

where n_1 and n_2 are the components of an eigen vector $\mathbf{n}$ that provides the orientation of the maximum stretch. This equation system has infinite solutions which correspond to vectors with the same direction (principal direction of λ_1). If we assume that $n_1 = 1$, we can determine the angle θ, that supplies this direction (Fig. 1). Making $n_1 = 1$ in the first of Eq. (9), we can find the value of n_2 using the equation:

$$n_2 = \tan\,\theta = \frac{(\lambda'_1 - c_{11})}{c_{12}} \tag{10}$$

Finally, the orientation of the lines of no finite deformation represented by the angle β (Fig. 1) is given by (Ramsay, 1967):

$$\tan^2\beta = \frac{(1 - \lambda'_1)}{(\lambda'_2 - 1)} \tag{11}$$

Different formats may be used to display the numerical results. To visualize the distribution and magnitude of deformation, the

ellipticity (ratio between the minimum and maximum elongation) obtained for each strain marker may be contoured using an interpolation algorithm such as kriging and the output should be overlapped on top of the present-day, deformed geological cross-section. This permits indentification, at a glance, zones of high deformation, their shape, location and relationships with the geological structure(s) analyzed. The orientation of the maximum elongation, minimum elongation and lines of no finite deformation may be displayed through lines properly oriented and positioned on the centre of each strain marker superposed on top of the present-day, deformed geological section across the structure(s) investigated.

The potential applicability and procedure of the method described is shown through its application to a section across a forward model of fault-propagation fold constructed using the classical Suppe and Medwedeff (1990) equations for constant thickness folds (Fig. 2a and b). Unlike natural structures, in this theoretical example there are no uncertainties related to the data and procedure employed in the geological cross-section construction, restoration and strain simulation. The deformation predicted across the structure is geologically reasonable and corresponds to that expected in this type of folds (Fig. 2c and d).

The main advantages of the methodology proposed are (a) it is not necessary to use specific software or particular equipment to

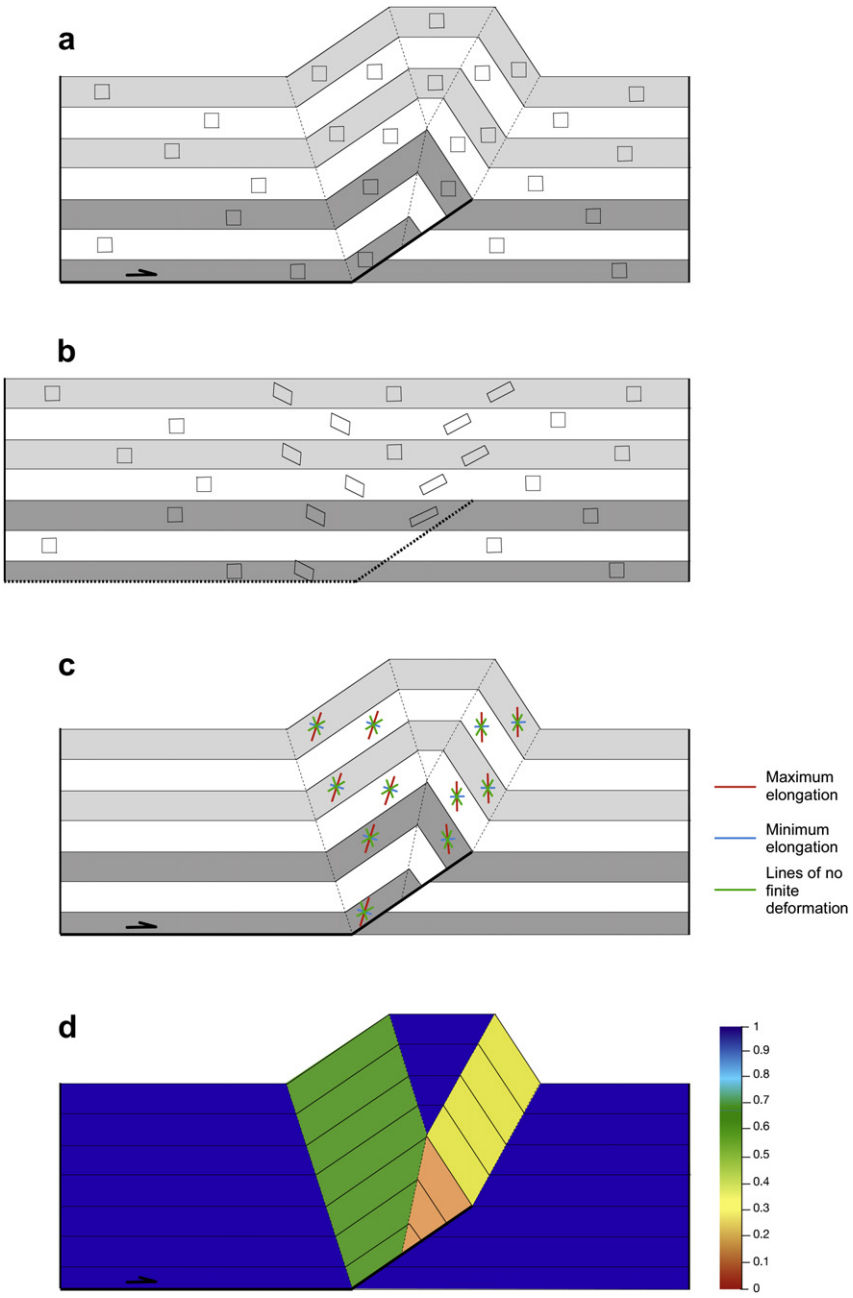

Fig. 2. Deformation simulation of a forward model of a parallel fault-propagation fold constructed using Suppe and Medwedeff (1990) equations. (a) Section across the fault-propagation fold including strain markers; (b) restoration of the section shown in (a); (c) orientation of maximum and minimum elongation and lines of no finite deformation for each strain marker; (d) magnitude of an ellipticity coefficient (minimum/maximum elongation ratio). The lengths of the elongation axes illustrated in (c) are the same for each strain marker and are not proportional to their values. In figure (d), the maximum deformation is represented by red colours with values tending to zero, whereas the minimum deformation is represented by blue colours with values close to one.

simulate deformation, since it can be modelled using a combination of conventional software to restore cross-sections and to perform data contouring and drawing packages; (b) the only parameters needed to perform the analysis are sections across structures and the strain markers placed arbitrarily on them; (c) the possibility of choosing the density, the size and the location of the strain markers allows us to obtain accurate results at any scale and in any structural position in relationship with the type, dimensions and geometry of the structure(s) analyzed; and (d) processing the deformation data using a mathematical model provides quantitative results and enables improving the technique at any time by including empirical corrections and/or more complex algorithms such as statistic filtering, etc.

3. Application of the method to a natural example

In order to test the validity of the method presented, it is applied to a contractional structure called Los Fuejos described below.

3.1. Geological setting

Los Fuejos structure is situated in the Cantabrian Zone (Fig. 3). The Cantabrian Zone is the external part of the Variscan orogen in northwest Iberian Peninsula and consists of a fold and thrust belt, developed during Carboniferous times. The structures exhibit a tight arcuate geometry in map view known as Ibero-Armorican or Asturian Arc, whereas in cross-sectional view they form an orogenic wedge that thins towards the foreland. The thrusts and related folds are consistent with a foreland-directed tectonic transport vector, however, some structures are overturned, so that they apparently moved towards the interior of the Cordillera (e.g., Julivert, 1971, 1979, 1981, 1983; Savage, 1979, 1981; Pérez-Estaún et al., 1988; Pérez-Estaún and Bastida, 1990; Aller et al., 2004 and references therein).

Los Fuejos structure is a several meters wide and high structure located in the north limb of a kilometric-scale, tight and approximately upright anticline whose axial plane strikes E–W and is called the Villasecino anticline (Fig. 3). This regional-scale anticline is interpreted to be a Variscan feature that deforms a number of Variscan folds and thrusts present in this region as can be observed in various geological maps (e.g., De Sitter, 1962; Marcos, 1968; Martínez-Álvarez et al., 1968; Alonso et al., 1989; Suárez-Rodríguez et al., 1990).

Los Fuejos structure is exposed in an approximately NNE–SSW section along a local road and involves Carboniferous limestones, radiolarites and shales (Fig. 4a and b). Only the central portion of the photograph shown in Fig. 4a, corresponding to red, fossil bearing, nodular limestones, has been studied. In particular, eight geological horizons were interpreted within this stratigraphic package. Overlying the limestones, to the north, there are red radiolarites detached from the limestones. Both, the red limestones and radiolarites belong to the Alba Formation. The lowermost interpreted horizon, to the south, where the basal detachment of Los Fuejos structure is located, consists of a thin level of black shales (Vegamián Formation) and constitutes the boundary between this formation and the white limestones of the underlying Baleas

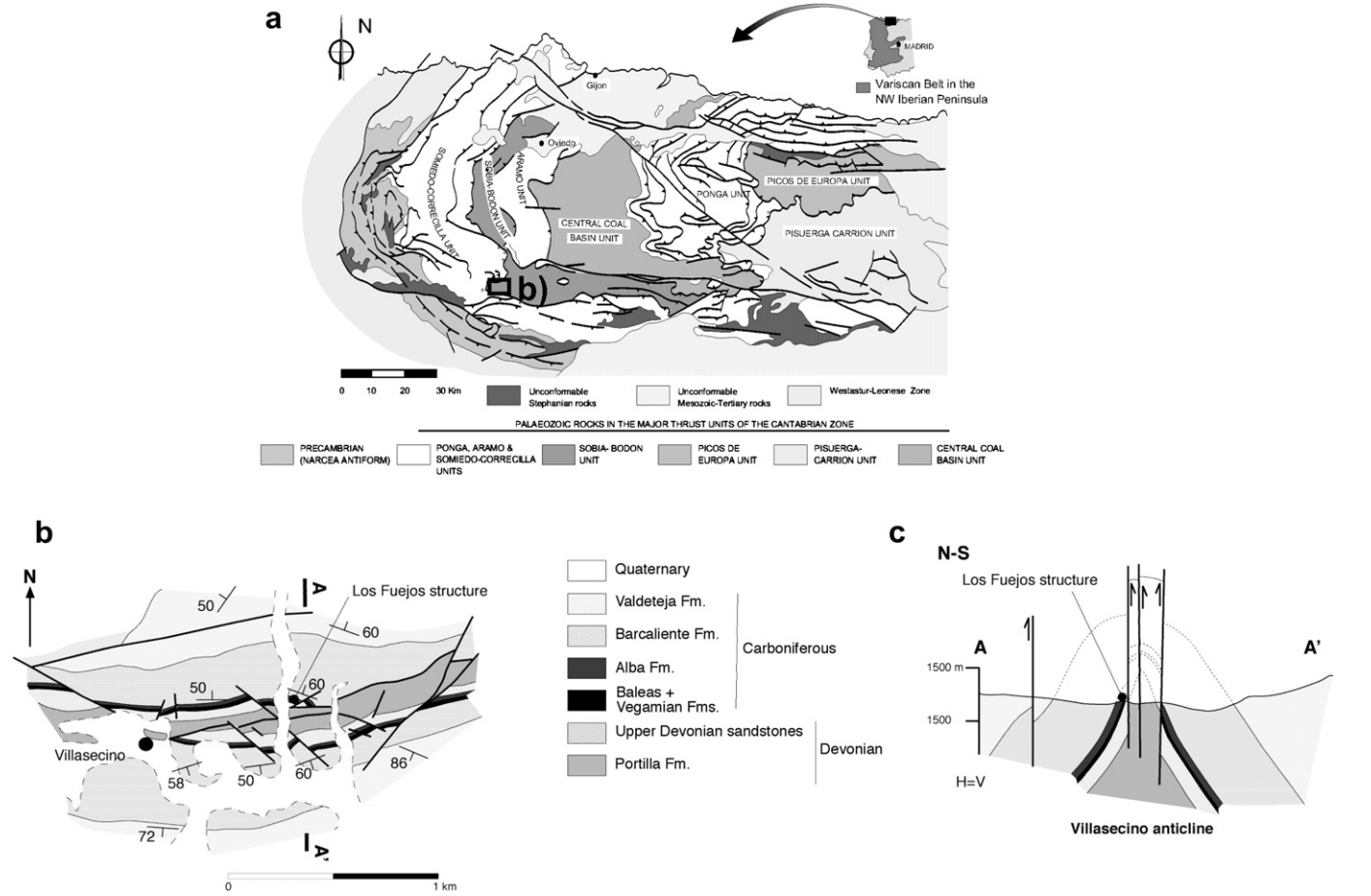

Fig. 3. (a) Structural sketch of the Cantabrian Zone (NW Iberian Peninsula) with location of the study area (southwest termination of the Bodón structural unit). (b) Geological map of the study area (modified from Suárez-Rodríguez et al., 1990). (c) Section A–A′ across the Villasecino anticline showing the position of Los Fuejos structure.

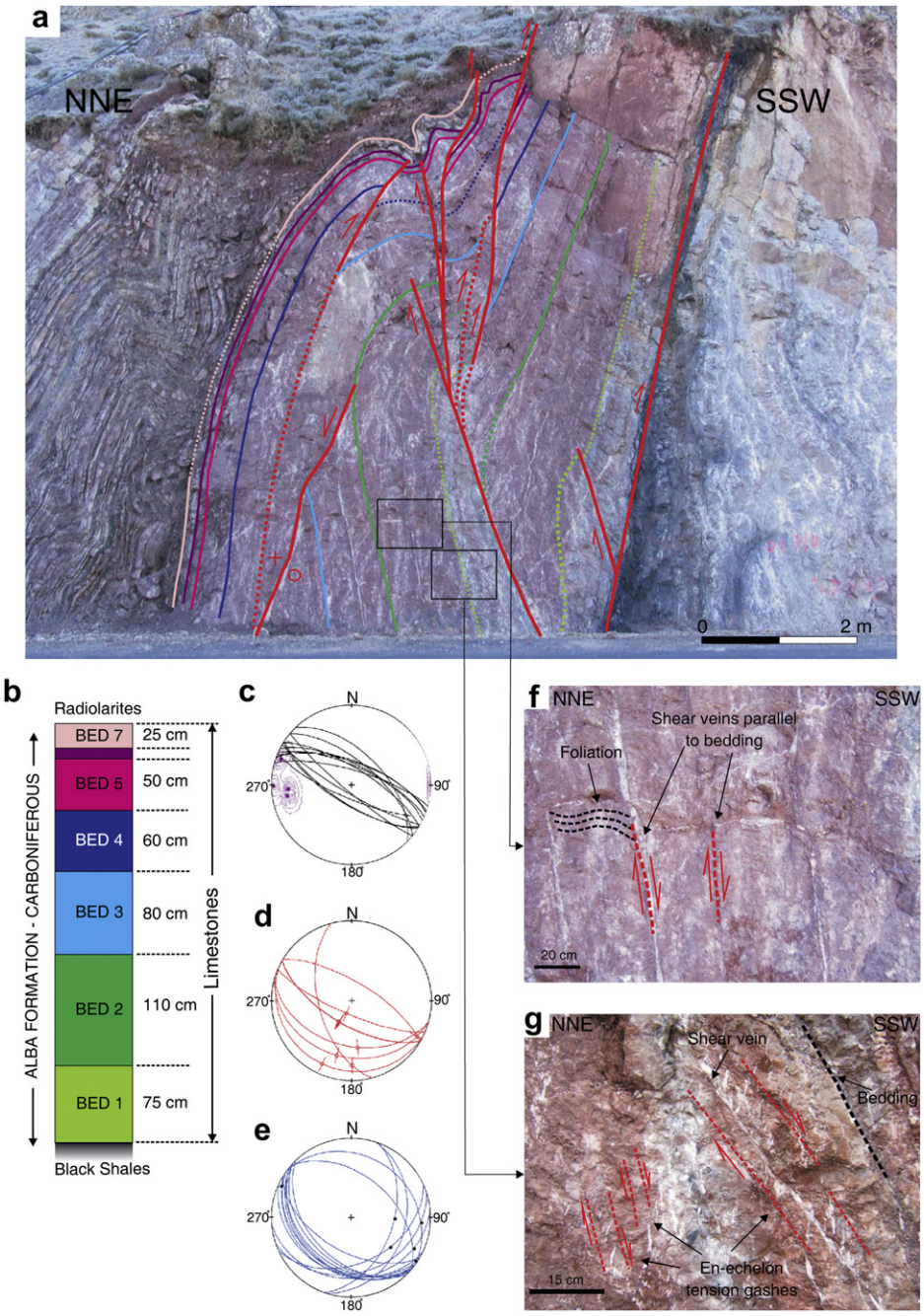

Fig. 4. (a) Geological interpretation of a photograph of Los Fuejos structure. (b) Stratigraphic section of the sedimentary sequence involved in the structure. (c) Equal area projection in the lower hemisphere of bedding (black lines) and fold axes (purple dots). (d) Equal area projection in the lower hemisphere of foliation (blue lines) and intersection lineations between foliation and bedding (black dots). (e) Equal area projection in the lower hemisphere of fault planes and slickensides. (f) Shear veins parallel to bedding and sigmoidal-shape foliation surfaces confined within them. (g) En-echelon tension gashes defining a band sub-parallel to bedding and shear vein slightly oblique to bedding compatible with the shear veins that bound a sigmoidal-shape foliation.

Formation of Upper Devonian–Carboniferous age (Alonso et al., 2008).

Los Fuejos structure is made up of folds and several faults. In outline, beds and structures strike in WNW-ESE direction and beds dip steeply towards the NNE (Fig. 4a and c). Folds have metric or smaller sizes, rounded hinges, approximately parallel geometry, interlimb angles around 90° and axial surfaces terminating against faults (Fig. 4a). Fold axes plunge sub-horizontally to gentle (Fig. 4c) and axial planes dip moderately to steeply towards the SSW. Stylolitic foliation surfaces dip moderately towards the SSW, however, they show occasional ENE–WSW strikes and moderate SSE dips (Fig. 4d). The variable orientation of the foliation surfaces is due to refraction and to the irregular foliation development in some limestone beds. The intersection lineations between bedding and foliation plunge gently to moderately towards the E and ESE (Fig. 4d). Except for the basal detachment, located between the Alba and Vegamián formations, faults are a few meters in length and this is also the maximum displacement along them, they are mainly oblique to bedding and constitute an imbricate fault system. They have a sub-vertical dip to both NNE and SSW (Fig. 4a and 4e), and, in cross-sectional view, exhibit normal and reverse movements.

Apart from folds and faults, several small-scale structures were observed: (a) bedding surfaces filled in by different generations of calcite parallel to the vein edges and elongated striations approximately perpendicular to the fold axis indicating that these bedding surfaces behaved as shear veins (Fig. 4f and g) (another generation of shear veins appears characterized by a sense of movement equivalent to that of the shear veins described above and slightly oblique to them); (b) a sigmoidal-shape foliation confined within the shear veins described above (Fig. 4f); (c) shear veins sub-perpendicular to bedding; (d) en-echelon tension gashes that define bands sub-parallel to bedding (Fig. 4g), and much less developed and less common conjugate bands of en-echelon tension gashes; and (e) a system of open fractures sub-perpendicular to bedding. In outline, most of the small-scale structures appear all over Los Fuejos structure, however, their development is much less intense in the outer part of the largest anticline hinge except for the open fractures restricted to this region. Single systems of en-echelon tension gashes occur in many places, however, conjugate systems mainly occur in the unfolded but tilted part of the structure located towards the south.

3.2. Construction of a cross-section

Los Fuejos structure is very well exposed enabling an accurate geological interpretation (Fig. 4a). The outcrop orientation is approximately parallel to the tectonic transport vector and approximately perpendicular to the strike of the structures. However, a proper visualization of the structure, a construction of a correct present-day cross-section and a subsequent cross-section restoration require modifications of the image shown in Fig. 4a described below.

(1) The geological interpretation of the photograph was corrected due to photographic distortions using a grid and accurate measurements of distances between grid nodes taken in the field.
(2) Los Fuejos structure is located in the north limb of the large-scale Villasecino anticline (Fig. 3), however, the temporal relationships between both structures are unknown; Los Fuejos structure could be developed: (a) before the initiation of the Villasecino anticline as a south-directed structure, or (b) during the Villasecino anticline amplification as a flexural-slip accommodation structure in its north limb. In any case, to better understand the relationships between beds, folds and faults, the geological interpretation of Los Fuejos structure was rotated 70° in a clockwise sense looking ESE around a horizontal ESE–WNW axis, until the detachment and the tilted black shales and light-coloured limestones, situated in the south side of Los Fuejos structure, became horizontal (Fig. 5a). The rotation performed consists of rotating the north limb of the Villasecino anticline as a rigid body. In the rotated geological section across Los Fuejos structure: (a) all the faults become reverse, (b) the detachment becomes horizontal, (c) the black shales and light-coloured limestones become the undeformed, flat-lying rocks located in the footwall of the structure, and (d) the geometrical relationships between folds and faults can be easily interpreted in terms of thrust-related folding in agreement with the structural style identified in surrounding areas.
(3) The next step consisted of constructing the sub-surface portion of the structure (Fig. 5a) using a technique called "projecting faults to depth" (Roeder et al., 1978) which consists of extrapolating the surface geological interpretation into the sub-surface using the available surface dip data, assuming that bed thickness remains constant and knowing the stratigraphic position of the detachment surface (sole thrust). Two different criteria were used to establish the stratigraphic position of the detachment: (a) a detachment between the Alba Fm. and the underlying Vegamián Fm. is observed in the outcrop at the base of Los Fuejos structure, and (b) the base of the Alba Fm. is a detachment surface in several portions of the Cantabrian Mountains (e.g., Julivert, 1983; Alonso, 1987; Bulnes and Marcos, 2001).
(4) The angle between the fold axis plunge and the outcrop surface is around 63°, and therefore, to visualize the structure properly, a fold profile perpendicular to the fold axis was obtained through a trigonometric correction assuming a constant plunge of the fold axis according to a procedure described by Ramsay and Huber (1987) (Fig. 5b).
(5) In the section obtained across Los Fuejos structure, a sub-horizontal, oblique to bedding fault occurs in the backlimb of the anticline (fault "g" in Fig. 5a). The geometry of this fault and its relationships with hangingwall and footwall beds suggest that it could be a north-northeast directed backthrust emanating from an anticline hinge. However, kinematic indicators,

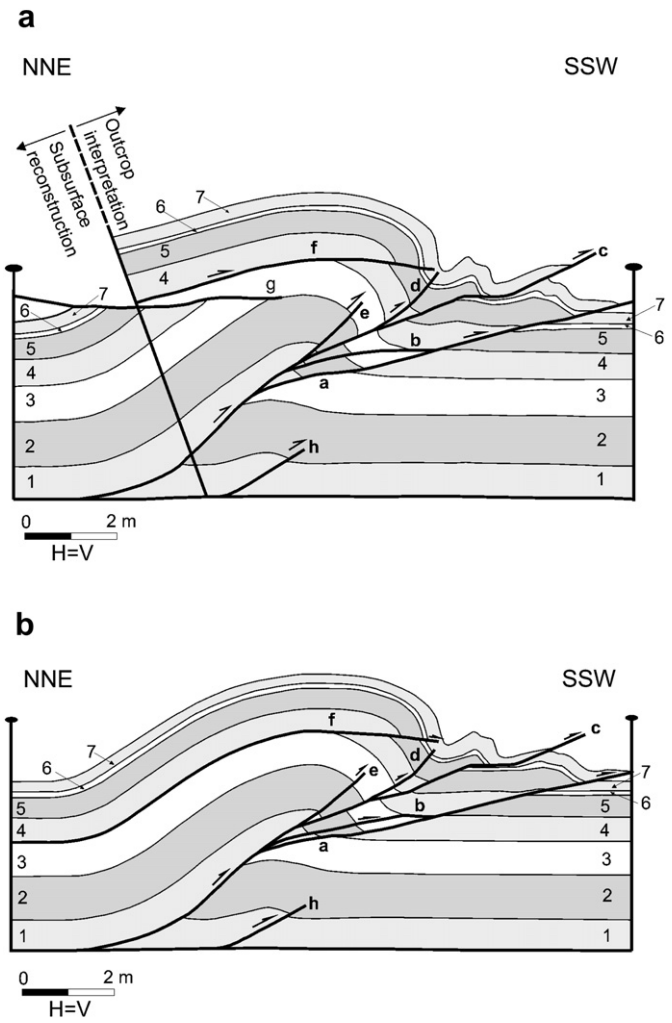

Fig. 5. (a) Reconstruction of a present-day cross-section using a photograph interpretation and outcrop measurements. The sub-surface portion is completed assuming that the thrust displays a hangingwall flat over a footwall ramp and branches with a basal detachment. (b) Final section across the Los Fuejos structure perpendicular to the main fold axis after the trigonometric correction of the cross-section displayed in a. In this section the fault "g" with strike-slip component was removed and this portion of the section was redrawn accordingly.

such as slickensides measured on the fault surface, point out that a main E–W strike-slip component of displacement took place along it. Since the cross-section obtained has to be restored, this fault was removed from the cross-section because it implies a certain amount of movement out of the section, approximately perpendicular to the main tectonic transport vector which will be described below. The beds in the hangingwall of this fault were redrawn in order to display a geologically reasonable reconstruction of the structure. The final section across Los Fuejos structure is presented in Fig. 5b.

3.3. Fault–.fold relationships and distribution of deformation within folded layers

In the profile across Los Fuejos structure, a thrust system formed by imbricate fault surfaces and a duplex is observed (faults "a", "b", "c", "d" and "e" in Fig. 5); individual fault surfaces dip from gently to moderately to the NNE, involve small amounts of displacement and usually display hangingwall ramps over footwall ramps. These minor thrusts emanate from a main thrust ramp that dips moderately to the NNE, exhibits a hangingwall flat over a footwall ramp and merges into a detachment surface that runs at the base of the Alba Fm. (Fig. 5). A second-order detachment at the base of bed 4 runs from the backlimb to the forelimb of the major anticline and becomes a small ramp segment in the hinge zone.

Folding is almost exclusively restricted to the hangingwall of the main thrust ramp except for a small thrust ramp in the footwall that dips moderately to the NNE, branches with the detachment and affects the two lowermost beds giving rise to a fault-related fold. The major fold is a metric-scale, open and asymmetric anticline with a large backlimb that dips gently to the NNE, and a shorter forelimb steeply dipping to the SSW. Decimetre-scale folding associated with the major anticline is located in its forelimb (Fig. 5).

The fold asymmetry (south-verging folds), the hangingwall and footwall thrust ramps and flats (Fig. 5), and some kinematic indicators, such as slickensides measured on the fault planes and asymmetric millimetre-scale folds developed in the black shales close to the detachment, point out a south-directed sense of tectonic transport.

The displacement along the imbricate thrust system decreases up section because shortening is taken up by folding. This can be observed in a displacement versus distance along a fault diagram (Fig. 6) constructed for fault "a" in Fig. 5 (the fault that exhibits the greatest displacement). Although the detailed interpretation of the displacement versus distance function is difficult because it depends on the rheology of the rocks (e.g., Muraoka and Kamata, 1983), type of fold (McConnell et al., 1997), occurrence of breakthroughs (Connors, pers. com.) and cut-off angles, the behaviour of the displacement/distance function points out that, stratigraphycally upwards, the displacement amount decreases. The loss of displacement along the faults stratigraphically upwards together with the following points: (a) asymmetric major anticline with a long, gently dipping backlimb, with a dip similar to that of the main thrust ramp, and a shorter, steeper forelimb, (b) relative small interlimb angle, (c) numerous second-order folds and imbricate thrusts in the forelimb and frontal syncline, and (d) thrusts whose tip point is located in the forelimb and frontal syncline indicates that the Los Fuejos structure can be interpreted as a fold-propagation fold related to an imbricate thrust system (Jamison, 1987; Suppe and Medwedeff, 1990; Mitra, 1990; Poblet, 2004 amongst others). The occurrence of fault-propagation folds in the Cantabrian Mountains has been documented in previous studies (e.g., Alonso and Marcos, 1992; Alonso and Teixell, 1992; Bulnes and Marcos, 2001; Bulnes and Aller, 2002).

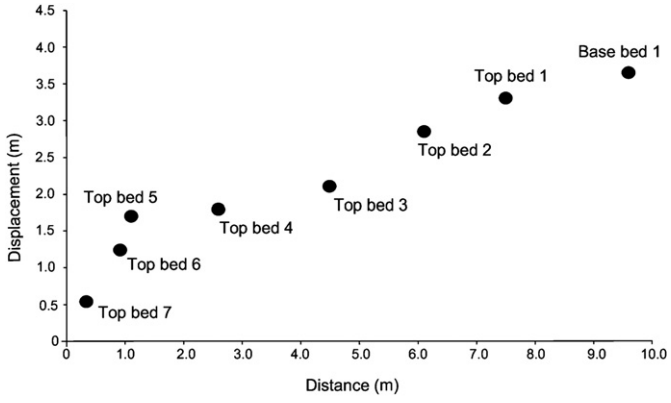

Fig. 6. Displacement versus distance graph constructed for fault "a" in Fig. 4.

The shear veins, the sigmoidal-shape foliation confined within the shear veins and the en-echelon tension gashes point out that layer-parallel shear occurred during fold amplification with displacement of each single bed towards the major anticline hinge relative to the underlying bed. Although there are evidences of layer-parallel shear as the main mechanism of distribution of deformation during Los Fuejos structure evolution, other mechanisms cannot be discarded. Thus, foliation, possibly originated by pressure/solution, and bed thickening in specific areas, for instance bed 7 in the forelimb of the major anticline (Fig. 5), suggest that layer-parallel shortening might have also occurred. The occurrence of open fractures in the outer part of the anticline hinge suggests that a component of tangential longitudinal extension might took place to a certain extent.

3.4. Cross-section restoration

The profile of Los Fuejos structure, approximately parallel to the tectonic transport and perpendicular to the fold axis (Fig. 7a), was restored to a pre-deformational stage to validate the geological interpretation, decipher the initial geometry of the structures and estimate the amount of shortening underwent by the structure (Fig. 7b). In order to restore the profile, a forward sequence of thrust emplacement was assumed.

A correct restoration of the section across Los Fuejos structure implies knowing the deformation mechanisms that operated in this particular structure in order to use appropriate algorithms. The small-scale structures described above indicate that layer-parallel shear seems to be the most plausible mechanism of distribution of deformation and explains the development of Los Fuejos structure. This led us to restore the cross-section using layer-parallel shear (software package Geosec 2D®). However, due to the complexity of the geological structure, employing exclusively one algorithm was not possible. It was necessary to integrate other algorithms in the restoration procedure such as equal-area balancing in some specific areas where evidence of layer-parallel strain exists. In particular, in the footwall of the main thrust ramp, there is a small-scale fold developed in beds number 1 and 2 linked to a thrust ramp (fault h in Fig. 5) where a thickness variation occurs. Another thickness variation involves beds number 5, 6 and 7.

The pin line (SSW end of the cross-section) was placed perpendicular to bedding in the transported along the detachment but unfolded footwall block, whereas the loose line (NNE end of the cross-section) was placed perpendicular to bedding in the unfolded but transported along the detachment hangingwall (Fig. 7a). The shortening values measured between the pin and loose lines in the restoration range from 3.18 to 4.53 m (19.1–25.2%) (Table 1).

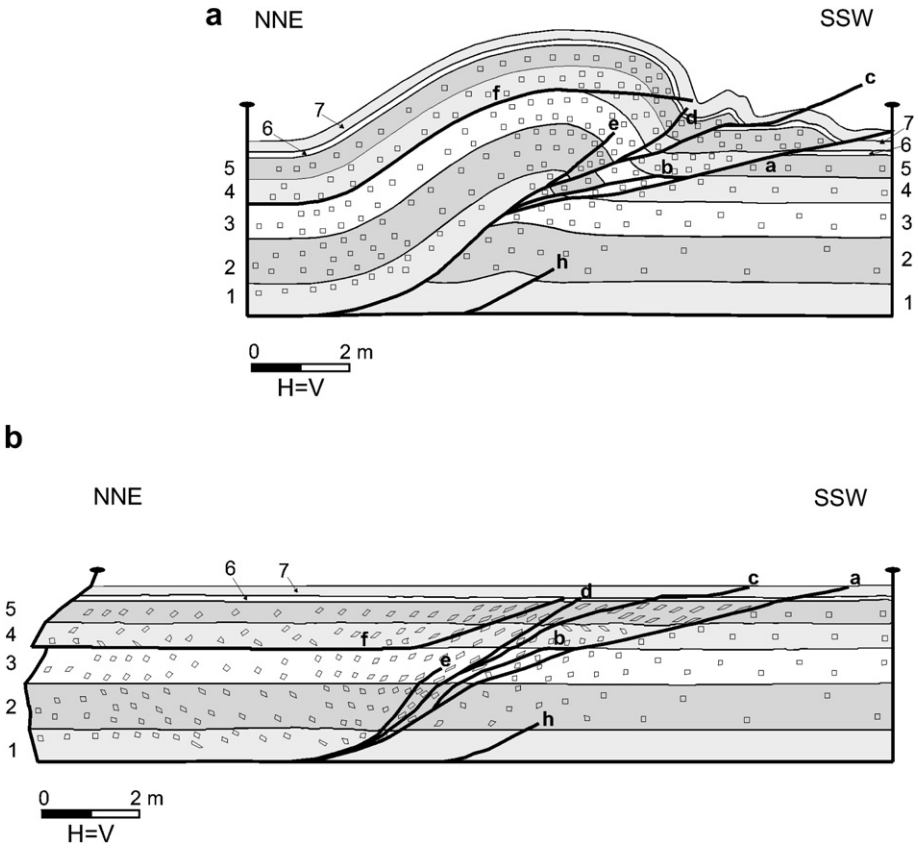

Fig. 7. (a) Balanced cross-section across the Los Fuejos structure and (b) restored section using the layer-parallel shear algorithm (and area restoration where local thickness variation occurs). In both the balanced section and the restoration, strain markers used to simulate the deformation are displayed.

The geometry of the restored loose line is irregular, dipping moderately to the NNE in the upper part of the stratigraphic sequence and steeply to the SSW in the lower part (Fig. 7b). This geometry may be the result of a certain amount of shear undergone by the structure. Nevertheless, major irregularities of the loose line occur within the beds affected by the fault with out-of-plane movement (fault "g" in Fig. 5a). The change in dip sense of the restored loose line takes place along the boundary between beds 2 and 3, where the tip of this fault is located. This suggests that, at least part of the irregularities of the loose line geometry might be the consequence of geometric modification of the Los Fuejos structure introduced when removing this fault from the cross-section.

The restoration achieved illustrates a detachment and an imbricate thrust system with ramps that dip around 10–30°; it is reasonable from the geological point of view, and therefore, it validates the geological interpretation of the structure.

Table 1
Shortening (in meters and in percentage) obtained from comparing the restoration of the profile across the Los Fuejos structure with the balanced profile.

Bed number	Length (m)	Shortening (m)	Shortening (%)
Top bed 7	16.63	3.18	19.1
Top bed 6	16.86	3.41	20.2
Top bed 5	17.03	3.58	21.0
Top bed 4	17.62	4.17	23.7
Top bed 3	17.84	4.39	24.6
Top bed 2	17.98	4.53	25.2
Top bed 1	17.92	4.47	25.0
Base bed 1	17.70	4.25	24.0

3.5. Deformation simulation

The adequacy of layer-parallel shear to restore most of the section across Los Fuejos structure allowed us to go on with the method to simulate the deformation presented above. The strain markers included in the section are the same size everywhere but their distribution is not homogeneous (Fig. 7a). The density, spacing and location of the markers were chosen to provide the best information about the strain architecture of this particular structure. Thus, there are only a few markers in the undeformed footwall, whereas the greatest density corresponds to the forelimb around the imbricate thrust system where the structures suggest a significant amount of deformation, and therefore, placing a large number of strain markers there is more relevant for deformation prediction. Nevertheless, part of bed 1, and beds 6 and 7 have no strain markers as no information can be obtained from these beds due to the algorithm employed to restore them, different from layer-parallel shear.

Fig. 8a shows the orientation of the axes of maximum and minimum elongation, and Fig. 8b displays the orientation of the lines of no finite deformation calculated from each strain marker. In the hangingwall block, close to the thrust ramp, the orientation of the elongation axes and lines of no finite deformation is compatible with small structures observed in the outcrop. The axes of maximum elongation (moderately plunging to the SSW in the anticline backlimb and moderately to steeply plunging to the SSW in the anticline forelimb in beds 3, 4 and 5, and steeply plunging to the NNE in beds 1 and 2) are sub-perpendicular to the tension gashes measured in the field; thus, the orientation of the axes of maximum elongation and the orientation of 61% of 18 tension

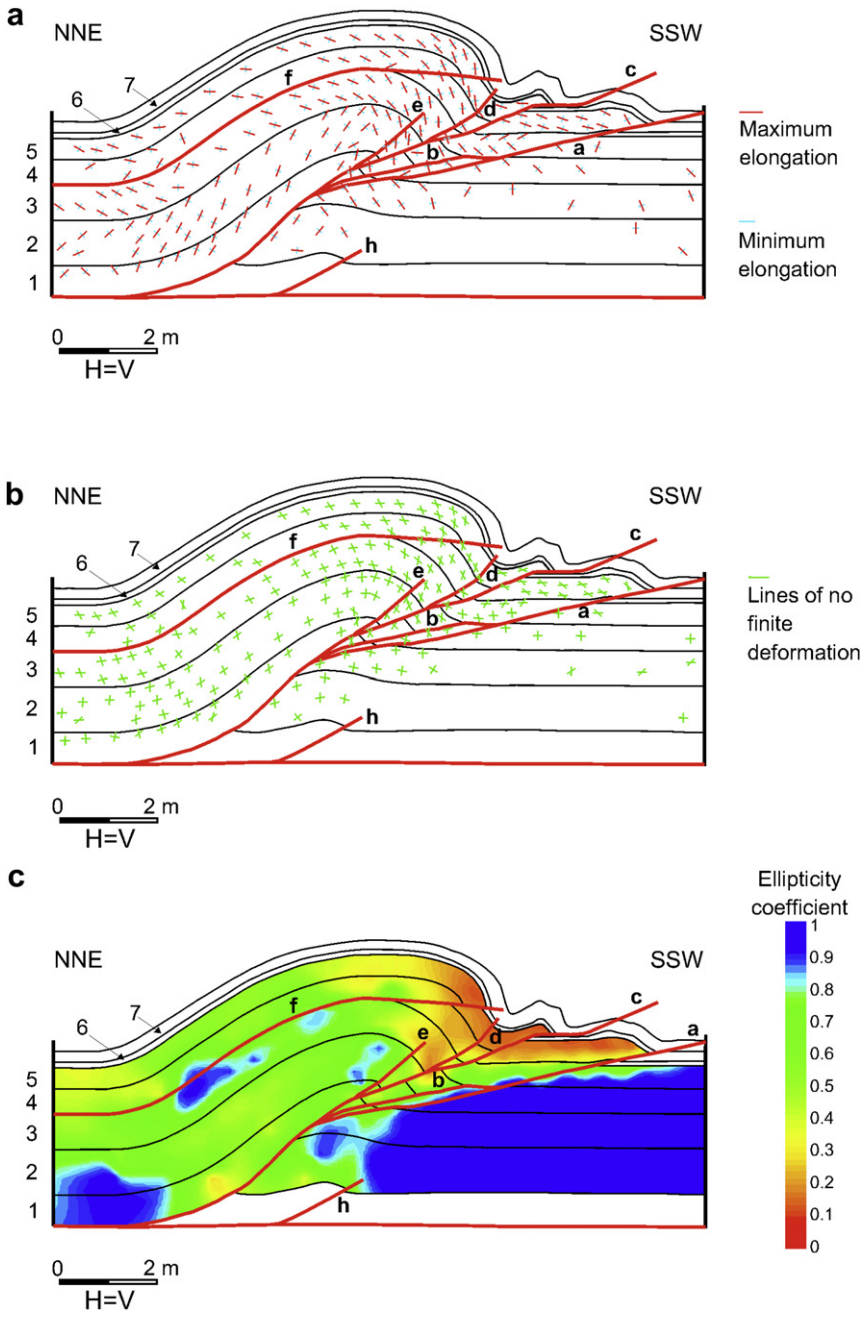

Fig. 8. Deformation simulation of the Los Fuejos fault-propagation fold including: (a) orientation of maximum and minimum elongation for each strain marker; (b) orientation of the lines of no finite deformation for each strain marker; (c) contours (obtained using the kriging interpolation algorithm) of an ellipticity coefficient (minimum/maximum elongation ratio) with the contour interval 0.02. The lengths of the elongation axes illustrated in (a) are the same for each strain marker and are not proportional to their values. In figure (c), the maximum deformation is represented by red colours with values tending to zero, whereas the minimum deformation is represented by blue colours with values close to one. The fact that the contours are not offset by the faults does not necessarily mean that ductile deformation postdates faulting, but to the superposition of the contours on top of the present-day cross-section.

gashes average from 80° to 90° apart, more than 33% of the tension gashes average from 70° to 80° apart, and 5.5% of the tension gashes average from 65° to 70° apart. The axes of minimum elongation are sub-perpendicular to the foliation surfaces observed; thus, the orientation of the axes of minimum elongation and the orientation of 60% of 15 foliation surfaces average from 80° to 90° apart, more than 13% of the foliation surfaces average from 70° to 80° apart, and more than 13% of the foliation surfaces average from 50° to 70° apart. In addition, the orientation of the axes of maximum and minimum elongation is consistent with the movement that occurred along bedding surfaces and bands defined by en-echelon tension gashes. In beds number 3, 4 and 5, located in the backlimb of the major anticline, the maximum and minimum elongation axes plunge in opposite senses with respect to the dips displayed in beds 1 and 2 (Fig. 8a). Such an anomaly, perhaps due to the geometric modification of Los Fuejos structure induced when the fault with out-of-plane movement was removed from the cross-section (fault "g" in Fig. 5a) and/or to the irregular geometry of the restored loose line (Fig. 7b), is not very important because of the small amount of deformation undergone by this area (Fig. 8c). However, such an anomaly would be consistent with the hypothesis of shear induced by fault "g" due to its displacement as

a backthrust. If correct, this would indicate that fault "g" was probably a backthrust reactivated as a strike-slip fault, but only strike-slip kinematic indicators were preserved.

One set of lines of no finite deformation is sub-parallel to bedding and to the bands defined by the en-echelon tension gashes measured in the field; thus, the average difference between the orientation of the predicted set of lines of no finite deformation and the orientation of 7 bands defined by en-echelon tension gashes varies from 0° to 10°. The other set of lines of no deformation forms a high angle with bedding and is sub-parallel to the conjugate bands of en-echelon tension gashes observed; thus, the average difference between the orientation of the predicted set of lines of no finite deformation and the orientation of 4 out of 5 conjugate bands defined by en-echelon tension gashes varies from 0° to 10°, and from 10° to 20° in the case of one of the conjugate bands. In the footwall block of the main thrust ramp, the low amount of deformation that affects this zone (Fig. 8c) does not permit a correct evaluation of the strain orientation (Fig. 8a) and this explains the slight dispersion of the elongation axes. The orientation of the maximum and minimum elongation axes and lines of no finite deformation in beds not offset by fault "g", i.e. beds 1 and 2 (Fig. 8a and 8b), is relatively similar to that observed in theoretical fault-propagation folds with constant bed thickness (lower part of Fig. 2c).

Fig. 8c shows contours constructed by interpolation of an ellipticity coefficient (minimum/maximum elongation ratio) derived from each strain marker on the reconstructed cross-section. The deformation distribution agrees with the field data and with the geological interpretation of Los Fuejos structure as a fault-propagation fold. Thus, the footwall block of the main thrust ramp, where bedding is horizontal and is not involved in the structure except for translation along a detachment, is characterized by a very low amount of deformation. To the south of the main thrust ramp, in the footwall block, there is an increment of deformation due to the small fold linked to thrust ramp "h". The maximum deformation is concentrated in the anticline forelimb, where beds dip steeply and an imbricate system occurs. The maximum deformation zone is approximately bounded by the forelimb-crest axial surface and the thrusts (Fig. 8c) as in theoretical parallel fault-propagation folds (Fig. 2d) and fault-propagation folds including combination of heterogeneous thrust-parallel simple shear and pure shear (Alonso and Teixell, 1992), and exhibits a triangular shape typical of many types of fault-propagation folds (Fig. 2d and e.g., Erslev, 1991; Alonso and Teixell, 1992; Allmendinger, 1998). The backlimb of the anticline, where beds dip gently and have been transported along the main thrust ramp, is characterized by moderate intensity of deformation that decreases towards the unfolded beds away from the structure.

4. Conclusions

The modelling technique presented, based on cross-section restoration, seems to successfully simulate deformation undergone by tectonic structures in 2D sections. We are aware, however, that to reach more solid conclusions this technique should be checked using examples developed in different tectonic settings, at various scales, with different amounts of shortening/extension, involving different materials, etc. The example analyzed here is just a first test.

The ability of this approach to simulate deformation makes it valuable to choose the correct structural interpretation in those situations in which several solutions are possible. Thus, applying this technique to all the possible sections across the structures and comparing the deformation simulations with second-order structures observed in the field, in seismic images, etc. may help to decide which is the best structural interpretation. This is particularly important from the purely scientific point of view and also in industry when the geometry and distribution of potential geological resources, the emplacement of infrastructures, etc. depend on structural controls.

Similarly to the methods described by De Paor (1990), Erickson et al. (2000), Hennings et al. (2000), Rouby et al. (2000), Dunbar and Cook (2003) and Poblet and Bulnes (2007), the technique presented here proves that cross-section restoration is a useful tool to predict the amount and distribution of deformation throughout folded/faulted rocks in addition to validating interpretations of structures by deciphering the original geometry and position of beds and structures, and quantifying the amount of contraction/extension.

The approach presented to simulate deformation patterns across tectonic structures requires few input parameters, i.e. a cross-section and the deformation mechanism, that are usually available. More complex algorithms could be incorporated into the technique to improve the results on the complex process of deformation in folded/faulted regions. However, complex models usually require more input parameters, which are difficult to obtain in many cases, and the predictive capabilities of the methods may become substantially reduced.

The structure analyzed in this paper, called Los Fuejos, involves Carboniferous limestones and occurs in the north limb of a regional-scale anticline in the Cantabrian fold and thrust belt (NW Iberian Peninsula). Field observations and the function obtained in a displacement versus distance diagram allowed us to classify this structure as a fault-propagation fold. The Los Fuejos structure developed during Variscan times prior to the regional-scale anticline or as a flexural-slip accommodation structure in the north limb of the regional-scale anticline during its amplification. Field evidences suggest that layer-parallel shear was the main mechanism that operated in Los Fuejos amplification, and therefore, layer-parallel shear was the algorithm employed to restore the section across the structure (plus equal-area balancing locally). The restoration carried out validated the geological interpretation and supplied shortening values comprised between 3.18 and 4.53 m (19.1–25.2%). According to the simulation of deformation performed, the maximum deformation occurred in a triangular zone located in the forelimb similar to many types of theoretical fault-propagation folds, whereas moderate deformation was recorded by the backlimb and almost negligible deformation in the almost undeformed footwall. The orientation of the strain parameters simulated (maximum and minimum elongation and lines of no finite deformation) is compatible with the type and orientation of the small-scale structures observed in the field (shear veins, en-echelon tension gashes and foliation surfaces).

The method proposed in this paper deals with kinematics but predicting accurately the features of different types of structures responsible for strain accommodation, specially brittle structures, demands a mechanical approach such as the geomechanical based restoration of Maerten and Maerten (2006) amongst others. However, a correspondence between outcrop mesostructures and the orientation of the strain markers simulated was found. This points out that the method presented might be used to suggest a full range of different types of small structures that accommodate strain in different portions of geological structures.

Acknowledgements

Suggestions by John Dunbar and Christopher Connors substantially improved the initial version of the manuscript. We also would

like to thank the editor Tom Blenkinsop, and Fernando Bastida, Nilo C. Bobillo-Ares, Juan Luis Alonso and Sabina Bigi for useful and constructive discussions. We acknowledge financial support by projects CGL2005-02233/BTE (3D modelling of folding kinematic mechanisms), CGL2008-03786/BTE (mechanical analysis of deformation distribution in folds), CGL2006-12415-C03-02/BTE (structural evolution of the Central Andes between parallels 23° and 33° during the Upper Paleozoic) and CSD2006-0041 (Topo-Iberia) under Consolider-Ingenio 2010 Programme funded by the Spanish Ministry for Education and Science, CGL2008-00463-E/BTE (International Meeting of Young Researchers in Structural Geology and Tectonics) funded by the Spanish Ministry for Science and Innovation, and CNG08-15 (International Meeting of Young Researchers in Structural Geology and Tectonics -YORSGET-08-) funded by the Asturian Ministry for Science and Education.

References

Aller, J., Álvarez-Marrón, J., Bastida, F., Bulnes, M., Heredia, N., Marcos, A., Pérez-Estaún, A., Pulgar, F.J.A., Rodríguez-Fernández, R., 2004. Estructura, deformación y metamorfismo (Zona Cantábrica). In: Vera, J.A. (Ed.), Geología de España. Sociedad Geológica de España-Instituto Geológico y Minero de España, Madrid, pp. 42–49.

Allmendinger, R.W., 1998. Inverse and forward numerical modelling of trishear fault-propagation folds. Tectonics 17, 640–656.

Allmendinger, R.W., Zapata, T., Manceda, R., Dzelalija, F., 2004. Trishear kinematic modelling of structures, with examples from the Neuquén Basin, Argentina. In: McClay, K.R. (Ed.), Thrust Tectonics and Hydrocarbon Systems. AAPG Memoir, vol. 82, pp. 356–371.

Alonso, J.L., 1987. Sequences of thrusts and displacement transfer in the superposed duplexes of the Esla Nappe region (Cantabrian zone, NW Spain). Journal of Structural Geology 9, 969–983.

Alonso, J.L., Álvarez-Marrón, J., Pulgar, F.J.A., 1989. Síntesis cartográfica de la parte sudoccidental de la Zona Cantábrica. Trabajos de Geología 18, 145–153.

Alonso, J.L., García-Alcalde, J.L., Aramburu, C., García-Ramos, J.C., Suárez, A., Martínez Abad, I., 2008. Sobre la presencia de la Formación Naranco (Devónico Medio) en el Manto de Bodón (Zona Cantábrica): implicaciones paleogeográficas. Trabajos de Geología 28, 159–169.

Alonso, J.L., Marcos, A., 1992. Nuevos datos sobre la estratigrafía y estructura de la Sierra del Pedrosu (Zona Cantábrica, NW de España): implicaciones tectónicas. Revista de la Sociedad Geológica de España 5, 81–88.

Alonso, J.L., Teixell, A., 1992. Forelimb deformation in some natural examples of fault-propagation folds. In: McClay, K.R. (Ed.), Thrust Tectonics. Chapman and Hall, London, pp. 175–180.

Bastida, F., Bobillo-Ares, N.C., Aller, J., Toimil, N.C., 2003. Analysis of folding by superposition of strain patterns. Journal of Structural Geology 25, 1121–1139.

Bulnes, M., Aller, J., 2002. Three-dimensional geometry of large-scale fault-propagation folds in the Cantabrian Zone, NW Iberian Peninsula. Journal of Structural Geology 24, 827–846.

Bulnes, M., Marcos, A., 2001. Internal structure and kinematics of Variscan thrust sheets in the valley of the Trubia River (Cantabrian Zone, NW Spain): regional tectonic implications. International Journal of Earth Sciences 90, 287–303.

Bulnes, M., Poblet, J., 1999. Estimating the detachment depth in cross sections involving detachment folds. Geological Magazine 136, 395–412.

De Paor, D.G., 1990. Cross-section balancing in space and time. In: Letouzey, J. (Ed.), Petroleum Tectonics in Mobile Belts. J. Letouzey and Editions Technip, Paris, pp. 149–154.

De Sitter, L.U., 1962. The structure of the southern slope of the Cantabrian Mountains. Geological map with section scale 1:100,000. Leidse Geologische Medelelingen 26, 255–264.

Dunbar, J.A., Cook, R.W., 2003. Palinspastic reconstruction of structure maps: an automated finite element approach with heterogeneous strain. Journal of Structural Geology 25, 1021–1036.

Dunnet, D., 1969. A technique of finite strain analysis using elliptical particles. Tectonophysics 7, 117–136.

Durney, D.W., Ramsay, J.G., 1973. Incremental strains measured by syntectonic crystal growth. In: DeJong, K.A., Scholten, R. (Eds.), Gravity and Tectonics. Wiley, New York, pp. 67–96.

Erickson, S.G., Hardy, S., Suppe, J., 2000. Sequential restoration and unstraining of structural cross sections: applications to extensional tectonics. AAPG Bulletin 84, 234–249.

Erslev, E.A., 1991. Trishear fault-propagation folding. Geology 19, 617–620.

Fry, N., 1979a. Random point distribution and strain measurement in rocks. Tectonophysics 60, 89–105.

Fry, N., 1979b. Density distribution techniques and strained line length method for determination of finite strain. Journal of Structural Geology 1, 221–229.

Hedlund, C.A., Anastasio, D., Fisher, D.M., 1994. Kinematics of fault-related folding in a duplex, Lost River Range, Idaho, U.S.A. Journal of Structural Geology 16, 571–584.

Hennings, P.H., Olson, J.E., Thompson, L.B., 2000. Combining outcrop data and three-dimensional structural models to characterize fractured reservoirs: an example from Wyoming. AAPG Bulletin 84, 830–849.

Jamison, W.R., 1987. Geometric analysis of fold development in overthrust terranes. Journal of Structural Geology 9, 207–219.

Julivert, M., 1971. Décollement tectonics in the Hercynian Cordillera of NW Spain. American Journal of Science 270, 1–29.

Julivert, M., 1979. A cross-section though the northern part of the Iberian Massif: its position within the Hercynian fold belt. Krystalinikum 14, 51–67.

Julivert, M., 1981. A cross-section though the northern part of the Iberian Massif. Geologie en Minbouw 60, 107–128.

Julivert, M., 1983. La estructura de la Zona Cantábrica. In: Comba, J.A., Libro Jubilar, JMRíos (Eds.), Geología de España. Tomo I. Instituto Geológico y Minero de España, Madrid, pp. 339–381.

Lisle, R.J., 1994. Detection of zones of abnormal strains in structures using Gaussian curvature analysis. AAPG Bulletin 78, 1811–1819.

Maerten, L., Maerten, F., 2006. Chronologic modeling of faulted and fractured reservoirs using geomechanically based restoration: technique and industry applications. AAPG Bulletin 90, 1201–1226.

Malvern, L.E., 1969. Introduction to the Mechanics of a Continuous Medium. Prentice-Hall, Englewood Cliff (New Jersey), 713 pp.

Marcos, A., 1968. La tectónica de la Unidad de La Sobia-Bodón. Trabajos de Geología 2, 59–87.

Martínez-Álvarez, J.A., Gutiérrez-Claverol, M., Vargas-Alonso, I., 1968. Esquema geológico de la zona de la Cordillera Cantábrica comprendida entre los Puertos "Pajares" y "Ventana" (Asturias-León). Cátedra de Geología, Escuela de Minas de Oviedo.

McConnell, D.A., Kattenhorn, S.A., Benner, L.M., 1997. Distribution of fault slip in outcrop-scale fault-related folds, Appalachian Mountains. Journal of Structural Geology 19, 257–267.

Mitra, S., 1990. Fault-propagation folds: geometry, kinematics and hydrocarbon traps. AAPG Bulletin 74, 921–945.

Moretti, I., Delos, V., Letouzey, J., Otero, A., Calvo, J.C., 2007. The use of surface restoration in Foothills exploration: theory and application to the Sub-Andean Zone of Bolivia. In: Lacombe, O., Lavé, J., Roure, F., Vergés, J. (Eds.), Thrust Belts and Foreland Basins. Springer, Berlin, pp. 149–162.

Muraoka, H., Kamata, H., 1983. Displacement distribution along minor fault traces. Journal of Structural Geology 5, 483–495.

Ormand, C.J., Hudleston, P.J., 2003. Strain paths of three small folds from the Appalachian Valley and Ridge, Maryland. Journal of Structural Geology 25, 1841–1854.

Pérez-Estaún, A., Bastida, F., 1990. Cantabrian Zone: structure. In: Dallmeyer, R.D., Martínez-García, E. (Eds.), Pre-mesozoic Geology of Iberia. Springer-Verlag, Berlin, pp. 55–69.

Pérez-Estaún, A., Bastida, F., Alonso, J.L., Marquínez, J., Aller, J., Álvarez-Marrón, J., Marcos, A., Pulgar, F.J.A., 1988. A thin-skinned tectonics model for an arcuate fold and thrust belt: the Cantabrian Zone (Variscan Ibero-Armorican Arc). Tectonics 7, 517–537.

Poblet, J., 2004. Geometría y cinemática de pliegues relacionados con cabalgamientos. Trabajos de Geología 24, 127–146.

Poblet, J., Bulnes, M., 2007. Predicting strain using forward modelling of restored cross-section: application to rollover anticlines over listric fault. Journal of Structural Geology 29, 1960–1970.

Ragan, D.M., 1985. Structural Geology: an Introduction to the Geometrical Techniques, third ed. Wiley, New York, 393 pp.

Ramsay, J.G., 1967. Folding and Fracturing of Rocks. McGraw-Hill, New York, 568 pp.

Ramsay, J.G., Huber, M.I., 1987. The Techniques of Modern Structural Geology. In: Folds and Fractures, vol. 2. Academic Press, London, 700 pp.

Roberts, A., 2001. Curvature attributes and their application to 3D interpreted horizons. First Break 19, 391–412.

Roeder, D., Gilbert, E., Witherspoon, W., 1978. Evolution of macroscopic structure of Valley and Ridge thrust belt, Tennessee and Virginia. Studies in Geology (Department of Geological Sciences, University of Tennesse) 2, 1–25.

Rouby, D., Xiao, H., Suppe, J., 2000. 3-D restoration of complexly folded and faulted surfaces using multiple unfolding mechanisms. AAPG Bulletin 84, 805–829.

Samson, P., Mallet, J.M., 1997. Curvature analysis of triangulated surfaces in structural geology. Mathematical Geology 29, 391–412.

Sanders, C., Bonora, M., Richards, D., Kozlowski, E., Sylwan, C., Cohen, M., 2004. Kinematic structural restorations and discrete fracture modeling of a thrust trap: a case study from the Tarija Basin, Argentina. Marine and Petroleum Geology 21, 845–855.

Savage, J.F., 1979. The hercynian orogeny in the cantabrian mountains, Northern Spain. Krystalinikum 14, 91–108.

Savage, J.F., 1981. Geotectonic cross-section through the cantabrian mountains, northern Spain. Geologie en Mijnbouw 81, 3–5.

Suárez-Rodríguez, A., Toyos, J.M., López-Díaz, F., Heredia, N., Rodríguez-Fernández, L.R., Gutiérrez-Alonso, G., 1990. Mapa geológico de España. Escala 1:50.000. Hoja: 102 (12–7) Los Barrios de Luna. Instituto Tecnológico y Geominero de España, Madrid, 130 pp.

Suppe, J., Medwedeff, D.A., 1990. Geometry and kinematics of fault propagation folding. Eclogae Geologicae Helvetiae 83, 409–454.

Thorbjornsen, K.L., Dunne, W.M., 1997. Origin of a thrust-related fold: geometric vs kinematic tests. Journal of Structural Geology 19, 303–319.